Analytical spectral density of the Sachdev-Ye-Kitaev model at finite N

Antonio M. García-García[1,*] and Jacobus J. M. Verbaarschot[2,†]

[1]Shanghai Center for Complex Physics, Department of Physics and Astronomy, Shanghai Jiao Tong University, Shanghai 200240, China

[2]Department of Physics and Astronomy, Stony Brook University, Stony Brook, New York 11794, USA

(Received 1 March 2017; published 11 September 2017)

We derive an approximate analytical formula for the spectral density of the q-body Sachdev-Ye-Kitaev (SYK) model obtained by summing a class of diagrams representing leading intersecting contractions. This expression agrees with that of Q-Hermite polynomials, with Q a nontrivial function of $q \geq 2$ and the number of Majorana fermions N. Numerical results, obtained by exact diagonalization, are in excellent agreement with this approximate analytical spectral density even for relatively small $N \sim 8$. For $N \gg 1$ and not close to the edge of the spectrum, we find that the approximate analytical spectral density simplifies to $\rho_{\mathrm{asym}}(E) = \exp[2\arcsin^2(E/E_0)/\log\eta]$, where $\eta(N,q)$ is the suppression factor of the contribution of intersecting Wick contractions relative to nested contractions and E_0 is the ground-state energy per particle. This spectral density reproduces the known result for the free energy in the large-q and large-N limit at arbitrary values of the temperature. In the infrared region, where the SYK model is believed to have a gravity dual, the analytical spectral density is given by $\rho(E) \sim \sinh[2\pi\sqrt{2}\sqrt{(1-E/E_0)/(-\log\eta)}]$. It therefore has a square-root edge, as in random matrix ensembles, followed by an exponential growth, a distinctive feature of black holes and also of low-energy nuclear excitations. Results for level statistics in this region confirm the agreement with random matrix theory. Physically this is a signature that, for sufficiently long times, the SYK model and its gravity dual evolve to a fully ergodic state whose dynamics only depends on the global symmetry of the system. Our results strongly suggest that random matrix correlations are a universal feature of quantum black holes and that the SYK model, combined with holography, may be relevant to modeling certain aspects of the nuclear dynamics.

DOI: 10.1103/PhysRevD.96.066012

I. INTRODUCTION

Majorana fermions in zero spatial dimensions with q-body infinite-range random interactions in Fock space, commonly termed Sachdev-Ye-Kitaev (SYK) models [1–11], are attracting a great deal of attention as one of the simplest strongly interacting systems with a possible gravity dual [12]. Previously, a closely related model with Majorana fermions replaced by Dirac fermions at finite chemical potential was intensively investigated in nuclear physics [13–18], and later in the study of spin liquids [19].

In the limit of a large number N of Majorana fermions, there is already a good understanding of many features of the model including thermodynamic properties [1,2,20], correlation functions [2,8,20], generalizations to nonrandom coupling [21], higher spatial dimensions and different flavors of Majorana fermions [10]. All evidence points to a gravity-dual interpretation [12] of the model in the low-temperature, strong-coupling limit. More specifically, it is believed that, in this limit, the gravity dual of the SYK model is related to an anti–de Sitter (AdS) background in two bulk dimensions, AdS_2 [5,11,22], which likely describes the low-energy sector of a string-theory dual to a gauge theory in higher dimensions. Related recent work can be found in Refs. [23–34].

One of the main appeals of the SYK model is the possibility to study explicitly finite N effects which are holographically dual to quantum gravity corrections [1,12]. Indeed, evidence for the existence of a SYK gravity dual is not restricted to large-N features such as a finite entropy at zero temperature or a finite specific heat coefficient but also includes properties controlled by subleading effects such as the exponential growth of the spectral density [2,35], the pattern of conformal symmetry breaking—or, for intermediate times of the order of the Ehrenfest time (a time scale of order $\log\hbar$ when quantum corrections start to affect substantially the classical motion, closely related to the scrambling time [36] originally introduced in the context of black hole physics), the universal exponential growth of certain out-of-time-ordered correlators [1,2,37]. The latter is also a well-known feature [38] of quantum chaos—namely, quantum features of classically chaotic systems.

Exponential growth of the spectral density together with random matrix correlations of the eigenvalues is a feature that is also well known in nuclear physics (see Refs. [39,40]), in particular for compound nuclei. These are

*amgg@sjtu.edu.cn
†jacobus.verbaarschot@stonybrook.edu

excited nuclei, where the energy of the incoming channel has been distributed over all nucleons. Because the dynamics is chaotic, all information on the formation of the compound nucleus is lost, and the quantum state is determined by the total energy and the exact quantum numbers. In this sense, a compound nucleus has no hair. However, it has "quantum hair" in the form of resonances which have been measured experimentally [41]. It turns out that fluctuations of the compound nucleus cross section obtained from these experiments agree well with random matrix theory predictions [42]. This implies that the S-matrix distribution is determined by causality or analyticity, ergodicity and the maximization of the information entropy [43].

Interestingly, qualitatively similar features have recently been found [35,44,45] for the SYK model. More specifically, the quantum chaotic nature of the model has been confirmed by showing that for long time scales, of the order of the Heisenberg time, level statistics are well described by random matrix theory [46,47]. The relation of this finding with features of the gravity dual has yet to be explored, as the analysis of spectral correlations carried out in these papers concerns the bulk of the spectrum and not the infrared tail related to the physics of the gravity dual. Moreover, the exponential growth of the SYK spectral density, a strong indication of the existence of a gravity dual, is based on a perturbative $1/N$ calculation [1,2] that may be spoiled by nonperturbative effects.

Here we address these two problems simultaneously. We obtain an analytical form for the spectral density of the q-body SYK model, for any q, by explicit evaluation of the moments for a large number of fermions, taking into account the leading intersecting contractions. The combinatorial factors are evaluated explicitly by using the Riordan-Touchard formula [48–50], derived originally in the theory of cords diagrams. We find that the moments of the density are equal to those of Q-Hermite polynomials [51], with $Q(N,q)$ a nontrivial function of N and q that we compute explicitly. Agreement with exact numerical results for $N \leq 34$ is excellent in spite of the $N \gg 1$ approximation involved in the analytical calculation. Our calculation follows the steps outlined in Ref. [52] for a closely related spin-chain model and in Ref. [35] of the SYK model, but we keep $q \geq 2$ fixed and $N \gg 1$ rather than considering the scaling limit $N \to \infty$ with q^2/N fixed studied in these papers. In the infrared limit, the spectral density has a square-root singularity, as in random matrix theory. Indeed, a detailed analysis of level statistics in this spectral region confirms excellent agreement with random matrix theory predictions. This suggests that, for sufficiently long times, a quantum black hole, characterized by fast scrambling [36], an exponential growth of low-energy excitations [53] and a finite Lyapunov exponent [37], reaches a fully ergodic and universal state which only depends on global symmetries of the system.

Finally, we note that the particular case $q/\sqrt{N}$ fixed and $N \to \infty$ was recently studied [35] for the SYK model, where the techniques of Ref. [52] were also employed to compute the infrared limit of the spectral density. In our result for the spectral density, which agrees with those of Ref. [35] in this limit, we do not take this double scaling limit for the contribution of the nonintersecting diagrams. Despite the approximations involved in the analytical result, the agreement with numerical results for $q = 4$, obtained by exact diagonalization for values of N as small as $N = 8$, is excellent.

Next, we introduce the model, compute analytically the spectral density, and compare it with numerical results. We close with concluding remarks and a discussion of our results.

II. MODEL AND CALCULATION OF THE SPECTRAL DENSITY

We study N strongly interacting Majorana fermions, introduced in Ref. [1], with infinite-range q-body interactions. For $q = 4$, the Hamiltonian is given by

$$H = \frac{1}{4!} \sum_{i,j,k,l=1}^{N} J_{ijkl} \chi_i \chi_j \chi_k \chi_l, \tag{1}$$

where χ_i are Majorana fermions that verify

$$\{\chi_i, \chi_j\} = 2\delta_{ij}. \tag{2}$$

We note that this is the same algebra as Dirac γ-matrices, which will facilitate the analytical evaluation of the moments. For that reason, we will use in many instances the notation γ to refer to the fields χ.

The coupling J_{ijkl} is a Gaussian random variable with probability distribution

$$P(J_{ijkl}) = \sqrt{\frac{N^{q-1}}{2(q-1)!\pi J^2}} \exp\left(-\frac{N^{q-1} J_{ijkl}^2}{2(q-1)! J^2}\right), \tag{3}$$

where J sets the scale of the distribution.

The average spectral density can be evaluated from the moment-generating function

$$\rho(E) = \frac{1}{2\pi} \int_{-\infty}^{\infty} dt\, e^{-iEt} \langle \mathrm{Tr} e^{iHt} \rangle, \tag{4}$$

where the brackets denote averaging over the probability distribution (3). Since the ensemble is invariant under $J \to -J$, we have that $\rho(-E) = \rho(E)$ so that the odd moments vanish. The moment-generating function, given by

$$\langle \mathrm{Tr} e^{iHt} \rangle = \sum_{k=0}^{\infty} \frac{(it)^{2k}}{(2k)!} \langle \mathrm{Tr} H^{2k} \rangle, \tag{5}$$

therefore follows from the moments

$$M_{2p} = \langle \mathrm{Tr} H^{2p} \rangle. \tag{6}$$

If we use the shorthand notation for the Hamiltonian

$$H = \sum_\alpha J_\alpha \Gamma_\alpha, \quad (7)$$

where Γ_α is the product of four γ-matrices, the moments are

$$\left\langle \mathrm{Tr}\left(\sum\nolimits_\alpha J_\alpha \Gamma_\alpha\right)^{2p}\right\rangle. \quad (8)$$

Since we have a Gaussian distribution, the calculation of the average requires us to consider all possible Wick contractions. After averaging, the result is given by a product of pairs of two factors Γ_α. If the factors are adjacent, we can use the fact that

$$\Gamma_\alpha^2 = 1. \quad (9)$$

If the factors are not adjacent, we have to commute the factors, using [45]

$$\Gamma_\alpha \Gamma_\beta - (-1)^{q+r} \Gamma_\beta \Gamma_\alpha = 0, \quad (10)$$

where r is the number of γ-matrices that Γ_α and Γ_β have in common. Generally, this is a difficult task, because we have to also keep track of correlations with other factors Γ_α, but the fourth, sixth, and eighth moments can be evaluated exactly [45].

The simplest case is the limit $N \to \infty$ for fixed p. To leading order in N, there are no common γ-matrices; the Γ_α commute and the moments are simply given by

$$\langle J_\alpha^2 \rangle^p 2^{N/2} (2p-1)!!, \quad (11)$$

which are the moments of a Gaussian distribution [45].

For large $N \gg 1$ but finite N, different Γ's have some γ-matrices in common. An exact analytical evaluation of an arbitrary high moment is a hard combinatorial task. We show below that the calculation is substantially simplified if one employs Eq. (10) to commute Γ factors but ignores correlations. Although we cannot justify rigorously the exact range of validity of the approximation, it is worth mentioning that for the low moments, where an explicit calculation is possible, this approximation is exact up to $1/N^2$ corrections. It is also exact [52] in the large-N limit with $q \propto N^\alpha$ and $\alpha > 1/2$. Moreover, we shall see that it leads to a spectral density that agrees well with exact diagonalization results even for small $N \geq 10$.

Let us consider

$$\mathrm{Tr}\Gamma_\alpha \Gamma_\beta \cdots \Gamma_\alpha \Gamma_\beta \cdots, \quad (12)$$

where the dots denote additional factors Γ_γ. We keep α fixed and consider the contribution from the sum over β. Commuting Γ_α and Γ_β gives a factor

$$\sum_{r=0}^{q} (-1)^{q+r} \binom{q}{r} \binom{N-q}{q-r}, \quad (13)$$

where r is the number of common χ fields which, as was mentioned previously, are represented by Dirac γ-matrices. Choosing them out of the q γ-matrices of Γ_α gives a factor $\binom{q}{r}$. The remaining $(q-r)$ γ-matrices in Γ_β still all have to be different from those in Γ_α. This gives a factor $\binom{N-q}{q-r}$, resulting in the combinatorial factor of Eq. (13). If Γ_α and Γ_β were commuting, the sum over β would give a factor $\binom{N}{q}$. Therefore, the suppression factor is given by

$$\eta_{N,q} = \binom{N}{q}^{-1} \sum_{r=0}^{q} (-1)^{q+r} \binom{q}{r} \binom{N-q}{q-r}. \quad (14)$$

For large N, at fixed q, only the $r = 0$ and $r = 1$ terms contribute to the sum of the suppression factor Eq. (14), resulting in

$$\eta \sim (-1)^q e^{-2q^2/N}, \quad (15)$$

where we have used that for $N \gg q$ we can make the expansion

$$\frac{\Gamma^2[N-q]}{\Gamma[N]\Gamma[N-2q]} = 1 - \frac{q^2}{N} + O(1/N^2). \quad (16)$$

This corresponds to the Poisson distribution used in Ref. [35].

The contractions contributing to the $2p$th moment can be characterized according to the number of crossings α_p. If there are α_p crossings, the diagram is suppressed by a factor $\eta_{N,q}^{\alpha_p}$. The sum over all crossings is evaluated by means of the Riordan-Touchard formula [48,49], resulting in the following expression for the moments:

$$\frac{M_{2p}}{M_2^p} = \sum_{\alpha_p} \eta_{N,q}^{\alpha_p} = \frac{1}{(1-\eta_{N,q})^p} \sum_{k=-p}^{p} (-1)^k \eta_{N,q}^{k(k-1)/2} \binom{2p}{p+k}. \quad (17)$$

These are the moments of the spectral density ρ_{QH} corresponding to the Q-Hermite polynomials with $Q = \eta$ [50–52]. Therefore, there is no need to calculate the Fourier transform of the moment-generating function in order to compute the spectral density in Eq. (4). The final result for the spectral density [52] of the SYK model [Eq. (1)] is

$$\rho(E) = \rho_{\mathrm{QH}}(E) = c_N \sqrt{1-(E/E_0)^2} \prod_{k=1}^{\infty} \left[1 - 4\frac{E^2}{E_0^2}\left(\frac{1}{2+\eta^k+\eta^{-k}}\right)\right], \quad (18)$$

where $\eta_{N,q} \equiv \eta$ is the suppression factor defined in Eq. (14), c_N is a normalization constant determined by imposing that the total number of states is $2^{N/2}$, and

$$E_0^2 = \frac{4\sigma^2}{1-\eta} \tag{19}$$

is the average value of the square of the ground-state energy per particle; i.e., the ground-state energy is NE_0, with the variance σ [45] given by

$$\sigma^2 = \binom{N}{q} \frac{J^2(q-1)!}{N^{q-1}}. \tag{20}$$

We note that the product in Eq. (18) can also be expressed in terms of a q-Pochhammer symbol. It is also valid for $\eta < 0$.

It is natural to ask for the precise requirements for the validity of Eq. (17). Corrections to this result arise when three or more factors Γ_α have one or more γ-matrices in common. Since this is a condition on two summation indices, this correction is expected to be of order $1/N^2$. We have worked out the exact analytical results for the fourth moment, which is identical to the Q-Hermite result; the sixth moment M_6/M_2^3 (see Ref. [45]); and M_8/M_2^4 for arbitrary q, and we have verified that indeed the difference with the moments (17) is of order q^3/N^2 and increases with the order of the moments (this scaling occurs for large values of $N \gg q^2$ where the moments are close to Gaussian). Exact results for higher-order moments are not known, but the results below indicate the moments Eq. (17) are close to the exact results. For example, for $N = 34$, the numerical result for the tenth moment differs by only 2% from the Q-Hermite result. However, $N = 34$ is still far from the large-N limit where the density is Gaussian: the eighth moment is only 25, as opposed to 105 for a Gaussian distribution.

In principle, large corrections to the analytical prediction above are still possible when the order of the moments becomes N. In general, high-order moments can have a strong impact on extreme eigenvalues which control the zero-temperature entropy and specific heat coefficient. However, as we will discuss below, our analytical results agree for all temperatures with the large-N, large-q limit of the partition function previously derived in Ref. [2].

Finally, we note that in Ref. [35], instead of using the exact suppression factor [Eq. (14)], η was approximated by a Poisson distribution, which is valid in the scaling limit where q^2/N is kept fixed [52] for $N \to \infty$, but not for general q.

Below we will show, by comparison to exact numerical results, that the above expression for the spectral density, with η given by Eq. (14), is close to the exact numerical result for $q = 4$, even for values of N as low as $N = 8$, where the suppression factor is negative. Before that, we work out simplifications of the spectral density [Eq. (18)] valid in the tail and the bulk of the spectrum.

III. SIMPLE FORM OF THE SPECTRAL DENSITY FOR $N \gg 1$

In this section, we derive a simple asymptotic form for the spectral density. The derivation follows the steps in Ref. [35], but we keep $q \geq 2$ fixed and do not take the limit $E \to E_0$. In this way we obtain an analytical form that can be applied to the entire spectrum of the Hamiltonian, except very close to the edge, and for any q with $\eta > 0$ with the only assumption of $N \gg 1$. For completeness, we reproduce the steps given in Ref. [35].

Writing the product in Eq. (18) as the exponent of a sum of logarithms, we obtain after a Poisson resummation

$$\rho_{\mathrm{QH}}(E) = c_N \exp\left[\frac{1}{2}\sum_{n=-\infty}^{\infty} \int dx e^{2\pi i n x} \log\left[1 - \frac{E^2}{E_0^2}\left(\frac{1}{\cosh^2 x/2 \log\eta}\right)\right]\right]. \tag{21}$$

The integral over x can be performed analytically, resulting in

$$\rho_{\mathrm{QH}}(E) = c_N \exp\left[-\frac{1}{2}\sum_{n=-\infty}^{\infty} \frac{1-\cosh[\frac{4n\pi}{\log\eta}\arcsin(E/E_0)]}{n\sinh(2n\pi^2/\log\eta)}\right]. \tag{22}$$

The $n = 0$ term in the sum has to be treated separately as the limit $n \to 0$. For $N \to \infty$, we have that $\eta \to 1$ so that for $n \neq 0$, we can approximate the hyperbolic functions by a single exponent, leading to

$$\begin{aligned}\rho_{\mathrm{Bethe}}(E) &= c_N \exp\left[\frac{2\arcsin^2(E/E_0)}{\log\eta} + \log\left(1 - \exp\left[-\frac{2\pi}{\log\eta}\left(|\arcsin(E/E_0)| - \frac{\pi}{2}\right)\right]\right)\right] \\ &= c_N \exp\left[\frac{2\arcsin^2(E/E_0)}{\log\eta}\right]\left(1 - \exp\left[-\frac{4\pi}{\log\eta}\left(|\arcsin(E/E_0)| - \frac{\pi}{2}\right)\right]\right).\end{aligned} \tag{23}$$

For $N \to \infty$, the second factor can be ignored for $|E| < |E_0|$, resulting in a very simple asymptotic form for the spectral density:

$$\rho_{\mathrm{asym}}(E) = c_N \exp\left[\frac{2\arcsin^2(E/E_0)}{\log \eta}\right], \tag{24}$$

which for finite $N \gg 1$ is an excellent approximation of the spectral density except in the region close to the edge E_0. Here a different asymptotic expression can be worked out by simply noticing that for $E \to E_0$, $\arcsin(x)$ is approximated by

$$\arcsin[E/E_0] = \frac{\pi}{2} - \sqrt{2}\sqrt{1-(E/E_0)}. \tag{25}$$

Inserting this into Eq. (23) gives

$$\rho_{\sinh}(E) \approx c_N \exp\left[\frac{\pi^2}{2\log\eta} - \frac{2\pi\sqrt{2}\sqrt{1-(E/E_0)}}{\log\eta}\right]\left(1 - \exp\left[\frac{4\pi}{\log\eta}\sqrt{2}\sqrt{1-(E/E_0)}\right]\right)$$
$$= 2c_N \exp\left[\frac{\pi^2}{2\log\eta}\right]\sinh\left[\frac{2\pi\sqrt{2}\sqrt{1-(E/E_0)}}{-\log\eta}\right]. \tag{26}$$

For the limiting case $q, N \to \infty$ with q^2/N fixed, and still $E \to E_0$, this expression of the spectral density was also obtained in Ref. [35].

We stress that this asymptotic form is an expected feature of field theories with a gravity dual, as this exponential growth is observed both in systems with conformal symmetry and in black holes [53]. The same exponential growth has also been predicted for the low-energy excitations of nuclei [54].

Having derived the approximate analytical result, we now proceed to compare the spectral densities [Eqs. (23) and (24)] with the exact Q-Hermite form [Eq. (18)]. Results depicted in Fig. 1 for different sizes N show that the simple asymptotic expression in Eq. (24) agrees reasonably well

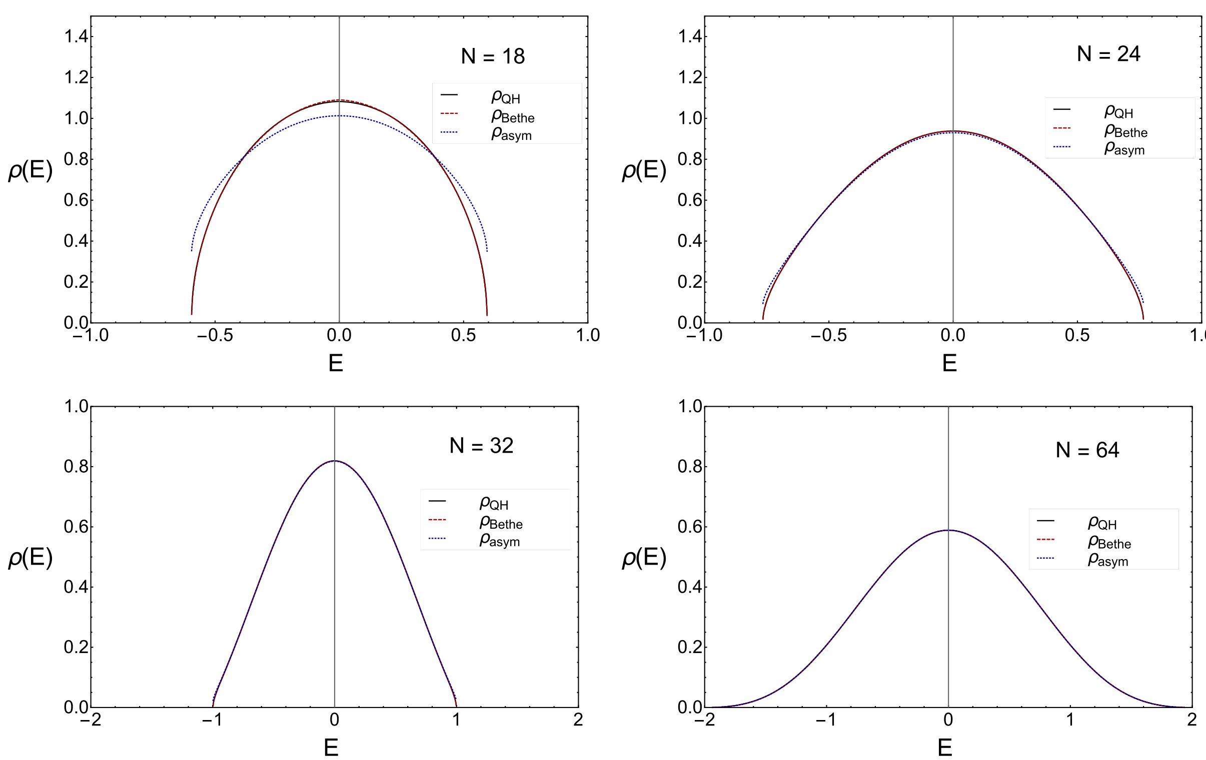

FIG. 1. We compare the Q-Hermite spectral density $\rho_{\mathrm{QH}}(E)$ [Eq. (18)] of the SYK Hamiltonian (black curve) to two different asymptotic forms, $\rho_{\mathrm{Bethe}}(E)$ [Eq. (23)] (red dashed curve) and $\rho_{\mathrm{asym}}(E)$ [Eq. (24)] (blue dotted curve), all normalized to area 1. Results are given for $N = 18$, $N = 24$, $N = 32$ and $N = 64$. For $N \geq 32$, the three curves are barely distinguishable. In all plots, the spectral density is normalized to 1 and $J = 2/3$. We note that this is also the value of J in our previous paper [45].

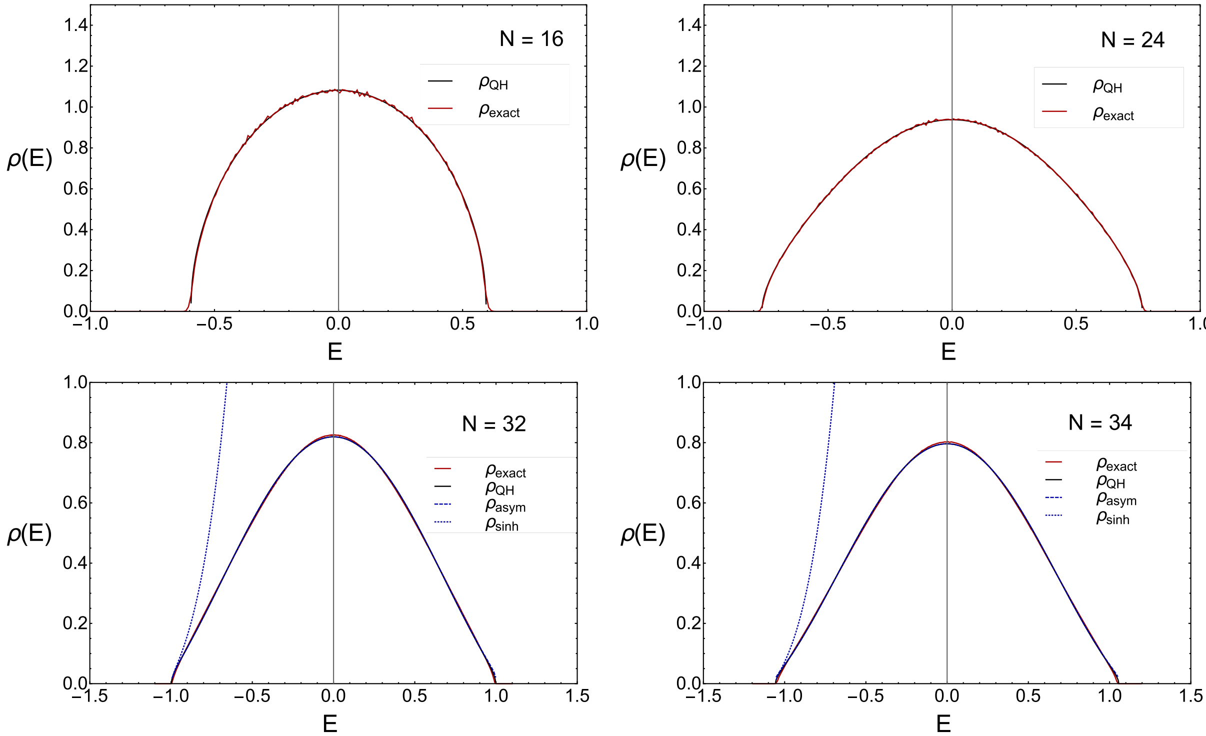

FIG. 2. Comparison of the numerical spectral density of the SYK Hamiltonian [Eq. (1)] (red) for $N = 16$, $N = 24$, $N = 32$ and $N = 34$, obtained by exact diagonalization, with the analytical prediction $\rho_{\mathrm{QH}}(E)$ [Eq. (18)] (black). In the bottom two figures, we also include $\rho_{\mathrm{asym}}(E)$ [see Eq. (24)], which is the large-N limit of $\rho_{\mathrm{QH}}(E)$, and $\rho_{\mathrm{sinh}}(E)$ [see Eq. (26)], which is the expansion of $\rho_{\mathrm{QH}}(E)$ near the edge of the spectrum. The agreement is excellent. Even though there are no free parameters, the curves are almost indistinguishable. As in the previous figure, the spectral density is normalized to 1 and $J = 2/3$.

with the exact result even for comparatively small $N = 18$. Indeed, it is barely distinguishable from the exact result in Eq. (18) for $N = 32$, while for $N = 64$ it can be used all the way to the edge of the spectrum.

We now proceed to compare these approximate analytical results with numerical results from exact diagonalization of the Hamiltonian [Eq. (1)]. By using standard exact diagonalization routines in MATLAB, we have obtained the full spectrum of the Hamiltonian [Eq. (1)] for many disorder realizations so that, for a given size $N \leq 34$, the total number of eigenvalues is more than 10^7. In Fig. 2, we show the exact numerical spectral density (red) and compare it to the analytical result [Eq. (18)] for $N = 16$, $N = 24$, $N = 32$ and $N = 34$. The agreement is excellent. For $N = 32$ and $N = 34$, we also show the large-N limit of $\rho_{\mathrm{QH}}(E)$ denoted by $\rho_{\mathrm{asym}}(E)$ and the form obtained from the expansion about $E = E_0$, which is denoted by $\rho_{\mathrm{sinh}}(E)$. We find that $\rho_{\mathrm{asym}}(E)$ is very close to the Q-Hermite result, while $\rho_{\mathrm{sinh}}(E)$ is only accurate for the extreme tail of the spectral density. Note that the analytical results do not have fitting parameters.

In order to further clarify the extent of the accuracy of the analytical spectral density, we extend the comparison to the deep infrared part of the spectrum (left plot of Fig. 3), where finite-size effects are expected to be more relevant.

The numerical density is still very close to the analytical prediction, but we have found some deviations. For instance, the hard edge predicted analytically is replaced by a smooth tail. Remarkably, the analytical edge of the spectrum [Eq. (19)] is still surprisingly close to the numerical result. Since not all subleading $1/N$ corrections were included in the derivation of the spectral density, stronger discrepancies were expected for the values of N we work with. It is actually rather unexpected that the analytical result is so close to the numerical calculation.

Still, we would like to understand why a tail, and not an edge, is observed in the numerical spectral density. We shall see in the next section that the level statistics of the model in this infrared region are still described by random matrix theory. We note that because of the stiffness of the spectrum, eigenvalues in random matrix theory fluctuate "collectively," which, due to ensemble average, smooths out the edge of the spectrum. This is particularly true for the lowest eigenvalue E_0, which is a stochastic variable, while the theoretical prediction Eq. (19) is the ensemble average. In order for a more accurate comparison, one has to either take into account the distribution of E_0 or simply remove the fluctuations of E_0. We choose the latter. In the right plot of Fig. 3, we show the spectral density relative to the first eigenvalue. To have the same scale on the x-axes, we have

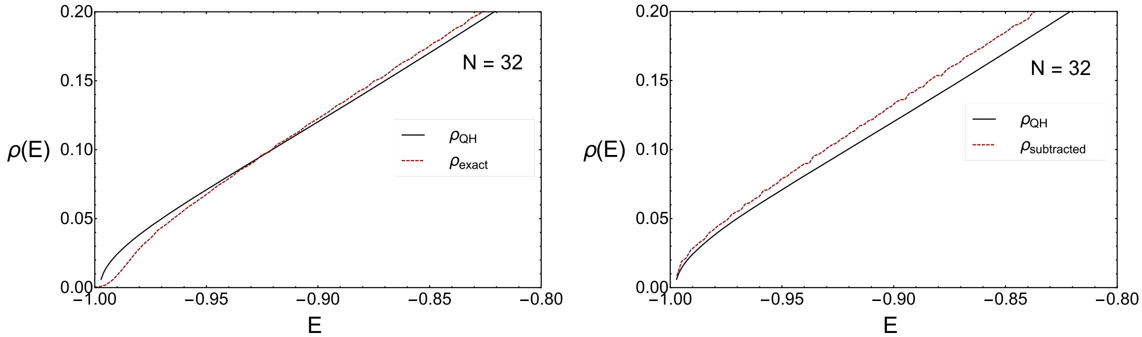

FIG. 3. The tail of the spectral density for $N = 32$ and 400 disorder realizations. In the right figure, $E_0 - \langle E_0 \rangle$ has been subtracted from all eigenvalues, while in the left figure no subtractions have been made. The agreement is excellent, despite the fact that finite-N effects, not fully captured in our theoretical analysis, should be stronger in this region. Even without this subtraction, the agreement is still very good.

added the ensemble average of the first eigenvalue to all eigenvalues. This clearly reveals the square-root edge of the average spectral density predicted theoretically.

This finding leads us to the prediction that the distribution of E_0 is the one given by random matrix theory for the distribution of the smallest eigenvalue—namely, the Tracy-Widom distribution [55]. In Fig. 4, we show the distribution of the smallest eigenvalue of the SYK model and compare it to the Tracy-Widom distribution of the corresponding random matrix ensemble. Results are given for $N = 24$ (left), which is in the universality class of the Gaussian orthogonal ensemble, and for $N = 28$ (right), which is in the universality class of the Gaussian symplectic ensemble. There are no fitting parameters, but the numerical data have been shifted and rescaled to reproduce the average and variance of the Tracy-Widom distribution. We find good agreement, which is another indication that the spectrum of the SYK Hamiltonian has a square-root edge.

We now employ the analytical form of the spectral density to study the free energy. We start with the density [Eq. (24)], which is valid everywhere except in the tail. The partition function in this case is given by

$$Z(\beta) = \int_{-E_0}^{E_0} dE\, c_N e^{-\beta E + \frac{2\arcsin^2(E/E_0)}{\log\eta}}. \tag{27}$$

For $\log\eta \to 0$, the partition function can be evaluated by a saddle-point approximation, resulting in the free energy

$$\beta F = \beta\bar{E} - \frac{2\arcsin^2(\bar{E}/E_0)}{\log\eta}, \tag{28}$$

where $\bar{E}$ satisfies the saddle-point equation

$$\beta = \frac{4}{E_0 \log\eta} \frac{\arcsin(\bar{E}/E_0)}{\sqrt{1-(\bar{E}/E_0)^2}}. \tag{29}$$

If we define the new variable

$$\arcsin\frac{\bar{E}}{E_0} = \frac{\pi v}{2}, \tag{30}$$

the saddle-point equation can be written as

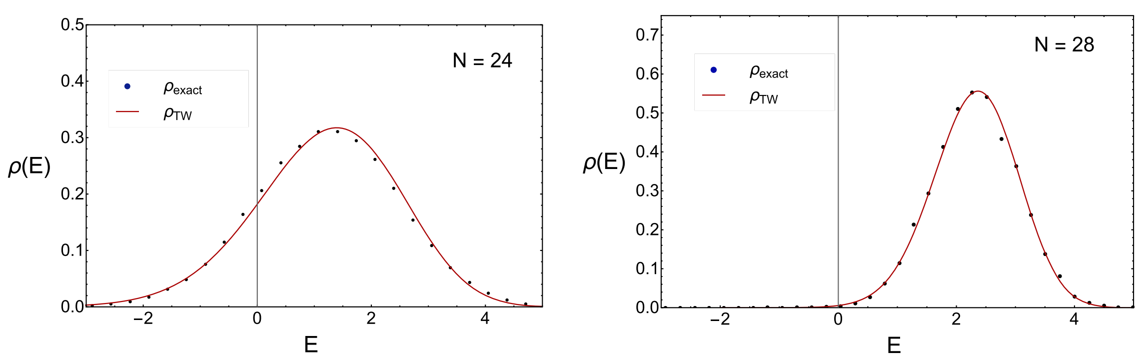

FIG. 4. Distribution of the lowest eigenvalue for $N = 24$ (left) and $N = 28$ (right) for ensembles of 50,000 and 15,000 disorder realizations, respectively, compared to the random matrix prediction for the Tracy-Widom distribution. The numerical data have been shifted and rescaled to reproduce the average and variance of the Tracy-Widom distribution. The agreement is excellent, which confirms that the low-energy limit of the SYK model is fully ergodic and well described by random matrix theory.

$$\beta\mathcal{J} = \frac{\pi v}{\cos\frac{\pi v}{2}}, \tag{31}$$

with $\mathcal{J} = (E_0/2)\log\eta$. In terms of these variables, the free energy at the saddle point is given by

$$\beta F = \frac{2}{\log\eta}\pi v \tan\frac{\pi v}{2} - \frac{(\pi v)^2}{2\log\eta}. \tag{32}$$

In the large-N limit, we have that $\log\eta \to -2q^2/N$, and this expression together with Eq. (31) reduces to the result derived in Ref. [2], which is obtained in the large-q limit for arbitrary values of the temperature. In the low-temperature limit, the fluctuations about the saddle point give a factor $1/\beta^{3/2}$, resulting in the low-temperature limit of the partition function [2]:

$$Z(\beta) \propto \beta^{-3/2}\exp\left[\beta|E_0| + \frac{N}{2}\log 2 + \frac{\pi^2}{2\log\eta} + \frac{2\pi^2}{\beta|E_0|\log^2\eta}\right]. \tag{33}$$

We note that the analytical evaluation of the partition function related to the tail of the spectrum [Eq. (26)], that includes $1/N$ corrections, reproduces this result identically.

In conclusion, the analytical form of the spectral density, which includes a class of $1/N$ corrections that results in moments which differ only at order $1/N^2$ from the exact result, agrees very well with exact numerical results. This is especially surprising close to the edge of the spectrum where higher-order $1/N$ effects, which have not been included in the theoretical analysis, are expected to be more relevant. We can only speculate that in systems with infinite-range interactions, a mean field approach becomes exact in the large-N limit and therefore, for finite N, fluctuations may be weaker than in systems with short-range interactions.

IV. APPLICATIONS IN NUCLEAR PHYSICS AND HOLOGRAPHY

The SYK and related models have been employed to study different aspects of nuclear physics, condensed matter and, more recently, holographic dualities. We now discuss how the results of the previous section help us better understand these systems. We start with holographic dualities. It was previously known [1,22] that $1/N$ corrections, combined with the saddle-point approximation, lead to a spectral density that grows exponentially for energies close, but not too close, to the ground-state energy. This is considered to be a distinctive feature of quantum black holes in the semiclassical limit and also in conformal field theories through the Cardy formula. Our results confirm this feature for any q, beyond the perturbative approach of Refs. [1,2]. In addition, it predicts—also for any $q > 2$—that $\rho(E) \sim \sqrt{E - E_0}$ for $E \to E_0$. This square-root edge,

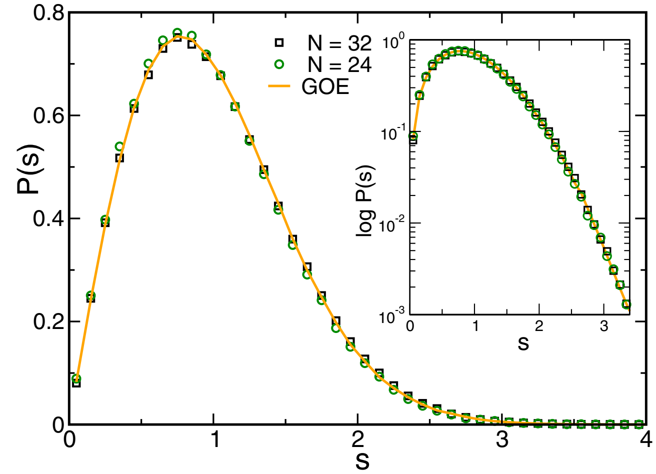

FIG. 5. Level spacing distribution $P(s)$ resulting from exact diagonalization of the SYK Hamiltonian [Eq. (1)] for $N = 32$ and 400 realizations (squares), and for $N = 24$ and 10000 realizations (circles). We only consider the infrared part of the spectrum, about 1.5%, which is related to the gravity dual of the model. As in the bulk of the spectrum [44,45], we observe excellent agreement with the Gaussian orthogonal ensemble (GOE) result. This strongly suggests that full ergodicity, typical of quantum systems described by random matrix theory, is also a universal feature of quantum black holes.

typical of random matrix ensembles, has been found in Refs. [35,52], but only in the slightly unphysical limit of $q \propto \sqrt{N}$.

In mesoscopic physics or quantum chaos, the occurrence of random matrix theory is related to full quantum ergodicity in the long time limit [47]—namely, the system evolves, for sufficiently long times, to a structureless and fully entangled state where only global symmetries characterize the dynamics. These are dynamical features, while the spectral density is only related to thermodynamical properties, which requires further checks to confirm quantum ergodicity of the SYK model and its gravity dual. For that purpose we have studied level statistics in the infrared region, where the spectral density is given by Eq. (26).

We note that level statistics of the SYK model have been studied previously [35,44,45]. However, these papers focus only on the central part of the spectrum that is not related to properties of the gravity dual. By contrast, we have studied the statistics of the low-lying eigenvalues—namely, the infrared part of the spectrum. Since we are interested in long-time dynamics of the order of the Heisenberg time, we investigate the level spacing distribution $P(s)$, defined as the probability to find two neighboring eigenvalues separated by a distance $s = (E_{i+1} - E_i)/\Delta$, where Δ is the mean level spacing Δ (see Ref. [45] for details of the calculation like the unfolding procedure). In Fig. 5, we depict results for $P(s)$ for $N = 24$ and $N = 32$, considering only 1.5% of the lowest eigenvalues. As in the central part of the spectrum [44,45], it follows closely the prediction of the Gaussian orthogonal ensemble (GOE). The good agreement shows that the eigenvalues of the SYK Hamiltonian fluctuate according to random matrix theory all the way to the ground-state region. This shows that the SYK Hamiltonian is chaotic in the infrared domain. This is a further confirmation of the full ergodicity of the SYK model in the long-time limit, and it is in agreement with the result of the previous section, that the distribution of the smallest eigenvalue is given by the Tracy-Widom distribution.

This is a strong indication that not only the SYK model but also its gravity dual, a certain type of quantum black hole, are systems whose long-time dynamics only depend on global symmetries and always lead to a completely featureless and ergodic quantum state. It is well known that random matrix ensembles are characterized by global symmetries only. It would be interesting to explore whether a similar classification characterizes the long-time dynamics of quantum black holes.

Nuclear physics is another area in which our results are of potential interest. A central feature of the excitations of complex nuclei is captured by Bethe's [54] expression that predicts an exponential growth of the density of states for energy close, but not too close, to the edge of the spectrum. Interestingly, the exponential growth predicted by the Bethe formula is very similar to that of Eq. (26). Experimental results agree, at least qualitatively, with this simple analytical expression. This is not fully understood, because interactions are typically strong, while Bethe's expression is derived assuming noninteracting fermions in a mean field potential. Our results help explain this puzzle, as the exponential growth also occurs in the SYK model, and likely in generalizations thereof, in which fermions are strongly interacting. This is also a strong indication that holography may be a powerful tool to model certain aspects of the physics of strongly interacting nuclei.

V. CONCLUSIONS

We have obtained an approximate analytical form for the spectral density of the SYK model which reproduces the large-q and large-N result for the partition function and agrees very well with numerical results for $q = 4$ and N as small as 8. This result was obtained by an explicit evaluation of the energy moments taking into account exactly a class of intersecting diagrams combined with the use of the Riordan-Touchard formula [48,49]. For moments of order $2p \ll N$, this approximation only differs at order $1/N^2$ from the exact result for the SYK model. For $N \gg 1$, and E not close to the ground state, the spectral density simplifies to $\rho_{\rm asym}(E) = \exp[2\arcsin^2(E/E_0)/\log\eta]$. In the infrared limit, the analytical expression for the spectral density has a square-root singularity, as in random matrix ensembles, followed by an exponential growth. Agreement with exact numerical results is excellent and is consistent with moments that are accurate including order-$1/N$ corrections. Our results also agree with the free energy in the large N, q limit studied in Ref. [2] by completely different methods though we do not make the assumption $q \gg 1$ in our analysis. We do not claim that the analytical spectral density, Eq. (18), is exact for any $q \geq 2$ up to corrections of order $1/N^2$, because moments of order N may have a different large-N scaling, and may contribute significantly to the tail of the spectrum. Nevertheless, we reproduce the zero-temperature entropy and low-temperature limit of the specific heat to leading order in $1/q^2$. Apparently, in the large-q limit, the correction to the large- order moments is suppressed. We hope to address this issue in a future publication.

We have also shown that level statistics in the infrared region are well described by random matrix theory for energy separations of the order of the Heisenberg time. Provided that the SYK model has a gravity dual in this quantum limit, our results indicate that, for sufficiently long times, quantum black holes relax universally to a fully ergodic and structureless state, where the dynamics is only dependent on the global symmetries of the system. These are exactly the properties of compound nuclei, which have a long history of being described in terms of random matrix theory.

ACKNOWLEDGMENTS

A. M. G. thanks Aurelio Bermúdez and Bruno Loureiro for illuminating discussions. This work acknowledges partial support from EPSRC Grant No. EP/I004637/1 (A. M. G.) and U.S. Department of Energy Grant No. DE-FAG-88FR40388 (J. V.).

[1] A. Kitaev, in KITP strings seminar and Entanglement 2015 program, http://online.kitp.ucsb.edu/online/entangled15/.
[2] J. Maldacena and D. Stanford, Phys. Rev. D **94**, 106002 (2016).
[3] J. Polchinski and V. Rosenhaus, J. High Energy Phys. 04 (2016) 001.
[4] J. Engelsöy, T. G. Mertens, and H. Verlinde, J. High Energy Phys. 07 (2016) 139.
[5] A. Almheiri and J. Polchinski, J. High Energy Phys. 11 (2015) 014.
[6] J. M. Magán, Phys. Rev. Lett. **116**, 030401 (2016).
[7] I. Danshita, M. Hanada, and M. Tezuka, arXiv:1606.02454.

[8] D. Bagrets, A. Altland, and A. Kamenev, Nucl. Phys. **B911**, 191 (2016).
[9] S. Sachdev, Phys. Rev. X **5**, 041025 (2015).
[10] D. J. Gross and V. Rosenhaus, J. High Energy Phys. 02 (2017) 093.
[11] K. Jensen, Phys. Rev. Lett. **117**, 111601 (2016).
[12] J. Maldacena, Int. J. Theor. Phys. **38**, 1113 (1999).
[13] O. Bohigas and J. Flores, Phys. Lett. **34B**, 261 (1971).
[14] O. Bohigas and J. Flores, Phys. Lett. **35B**, 383 (1971).
[15] J. French and S. Wong, Phys. Lett. **33B**, 449 (1970).
[16] J. French and S. Wong, Phys. Lett. **35B**, 5 (1971).
[17] V. Kota, Phys. Rep. **347**, 223 (2001).
[18] L. Benet and H. A. Weidenmller, J. Phys. A **36**, 3569 (2003).
[19] S. Sachdev and J. Ye, Phys. Rev. Lett. **70**, 3339 (1993).
[20] A. Jevicki, K. Suzuki, and J. Yoon, J. High Energy Phys. 07 (2016) 007.
[21] E. Witten, arXiv:1610.09758.
[22] J. Maldacena, D. Stanford, and Z. Yang, Prog. Theor. Exp. Phys. **2016**, 12C104 (2016).
[23] M. Berkooz, P. Narayan, M. Rozali, and J. Simón, J. High Energy Phys. 01 (2017) 138.
[24] W. Fu, D. Gaiotto, J. Maldacena, and S. Sachdev, Phys. Rev. D **95**, 026009 (2017).
[25] I. R. Klebanov and G. Tarnopolsky, Phys. Rev. D **95**, 046004 (2017).
[26] T. Nishinaka and S. Terashima, arXiv:1611.10290.
[27] C. Peng, M. Spradlin, and A. Volovich, J. High Energy Phys. 05 (2017) 062.
[28] Y. Liu, M. A. Nowak, and I. Zahed, arXiv:1612.05233.
[29] G. Turiaci and H. Verlinde, arXiv:1701.00528.
[30] J. M. Magan, arXiv:1612.06765.
[31] A. R. Kolovsky and D. L. Shepelyansky, Europhys. Lett. **117**, 10003 (2017).
[32] S. Banerjee and E. Altman, Phys. Rev. B **95**, 134302 (2017).
[33] C. Krishnan, S. Sanyal, and P. N. B. Subramanian, J. High Energy Phys. 03 (2017) 056.
[34] H. Kyono, S. Okumura, and K. Yoshida, J. High Energy Phys. 03 (2017) 173.
[35] J. S. Cotler, G. Gur-Ari, M. Hanada, J. Polchinski, P. Saad, S. H. Shenker, D. Stanford, A. Streicher, and M. Tezuka, J. High Energy Phys. 05 (2017) 118.
[36] Y. Sekino and L. Susskind, J. High Energy Phys. 10 (2008) 065.
[37] J. Maldacena, S. H. Shenker, and D. Stanford, J. High Energy Phys. 08 (2016) 106.
[38] A. Larkin and Y. N. Ovchinnikov, Sov. Phys. JETP **28**, 1200 (1969).
[39] T. von Egidy, A. N. Behkami, and H. H. Schmidt, Nucl. Phys. **A454**, 109 (1986).
[40] R. U. Haq, A. Pandey, and O. Bohigas, Phys. Rev. Lett. **48**, 1086 (1982).
[41] J. B. Garg, J. Rainwater, J. S. Petersen, and W. W. Havens, Phys. Rev. **134**, B985 (1964).
[42] J. J. M. Verbaarschot, H. A. Weidenmuller, and M. R. Zirnbauer, Phys. Rep. **129**, 367 (1985).
[43] P. A. Mello, P. Pereyra, and T. H. Seligman, Ann. Phys. (N.Y.) **161**, 254 (1985).
[44] Y.-Z. You, A. W. W. Ludwig, and C. Xu, Phys. Rev. B **95**, 115150 (2017).
[45] A. M. García-García and J. J. M. Verbaarschot, Phys. Rev. D **94**, 126010 (2016).
[46] F. Dyson, J. Math. Phys. (N.Y.) **3**, 140 (1962).
[47] T. Guhr, A. Mueller-Groeling, and H. A. Weidenmueller, Phys. Rep. **299**, 189 (1998).
[48] J. Touchard, Can. J. Math. **4**, 2 (1952).
[49] J. Riordan, Math. Comput. **29**, 215 (1975).
[50] P. Flajolet and M. Noy, *Formal Power Series and Algebraic Combinatorics: 12th International Conference, FPSAC'00, Moscow, Russia, June 2000*, edited by D. Krob, A. A. Mikhalev, and A. V. Mikhalev (Springer, Berlin, Heidelberg, 2000), pp. 191–201.
[51] M. E. Ismail, D. Stanton, and G. Viennot, Eur. J. Combinatorics **8**, 379 (1987).
[52] L. Erdős and D. Schröder, Math. Phys. Anal. Geom. **17**, 9164 (2014).
[53] S. Carlip, Classical Quantum Gravity **17**, 4175 (2000).
[54] H. A. Bethe, Phys. Rev. **50**, 332 (1936).
[55] C. A. Tracy and H. Widom, Commun. Math. Phys. **159**, 151 (1994).